

# NL-SLAM for OC-VLN: Natural Language Grounded SLAM for Object-Centric VLN

Sonia Raychaudhuri<sup>1,2</sup>, Duy Ta<sup>1</sup>, Katrina Ashton<sup>1,3</sup>, Angel X. Chang<sup>2</sup>, Jiuguang Wang<sup>1</sup>, Bernadette Bucher<sup>1,4</sup>

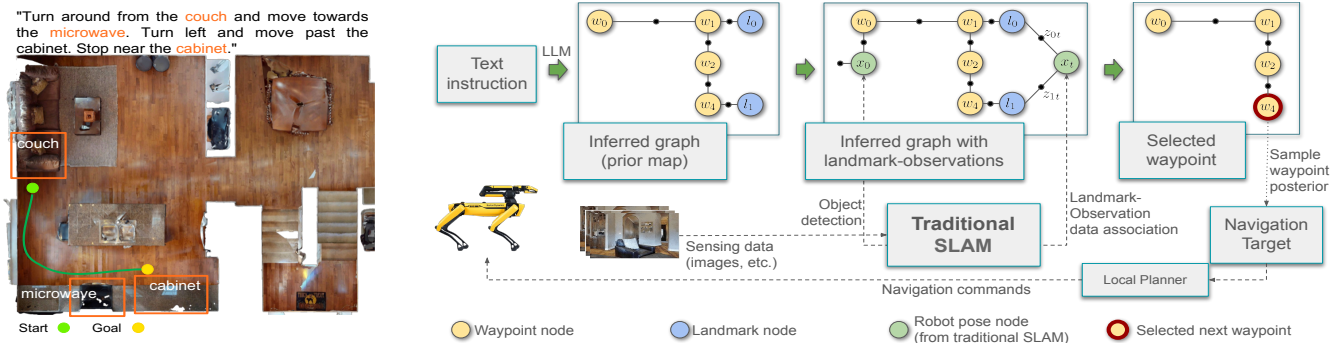


Fig. 1: We propose OC-VLN dataset with object-centric free-form language instructions (left), and NL-SLAM to ground natural language instructions to robot observations and poses to actively follow instructions to perform navigation (right).

**Abstract**—Landmark-based navigation (e.g., go to the wooden desk) and relative positional navigation (e.g., move 5 meters forward) are distinct navigation challenges solved very differently in existing robotics navigation methodology. We present a new dataset, OC-VLN, in order to distinctly evaluate grounding object-centric natural language navigation instructions in a method for performing landmark-based navigation. We also propose Natural Language grounded SLAM (NL-SLAM), a method to ground natural language instructions to robot observations and poses. We actively perform NL-SLAM in order to follow object-centric natural language navigation instructions. Our methods leverage pre-trained vision and language foundation models and require no task-specific training. We construct two strong baselines from state-of-the-art methods on related tasks, Object Goal Navigation and Vision Language Navigation, and we show that our approach, NL-SLAM, outperforms these baselines across all our metrics of success on OC-VLN. Finally, we successfully demonstrate the effectiveness of NL-SLAM for performing navigation instruction following in the real world on a Boston Dynamics Spot robot. The OC-VLN dataset, code, and videos are available at [sonia-raychaudhuri.github.io/nlslam](https://sonia-raychaudhuri.github.io/nlslam).

## I. INTRODUCTION

Humans perform visual navigation by using landmarks to determine where they are in the world. Landmarks are distinctive sites in a scene such as objects or topological features (e.g., a particular tree or building). While we can understand relative movement from our current location (e.g., move 5 meters forward), grounding this spatial understanding in landmarks is required to understand our placement in

larger regions (e.g., now I am by the front door) [1]–[4]. To follow navigation instructions, humans associate landmarks described in natural language with real landmarks observed in the environment to simultaneously understand where they are in the instruction and in the world.

Roboticians studying mapping and navigation have developed methods for creating landmark maps from visual observations and using those maps for autonomous navigation [5]–[11]. In fact, work in this area has matured far enough to move beyond the research community. Landmark-based mapping and navigation systems are widely used in autonomous robot operation in many industry applications, including home robot vacuum cleaners [12], [13] and drones for surveying and inspection [14]. With recent advances in natural language understanding due to large language and vision-language models [15]–[20], the next frontier is to determine how to accurately align natural language navigation instructions with observation-based autonomous decision making capabilities in these mature robotic systems.

To support research in this direction, researchers have developed benchmarks for evaluating an autonomous agent’s ability to follow natural language navigation instructions in simulation, specifically R2R [21], RxR [22], and VLN-CE [23]. These benchmarks consist of datasets of natural language instructions and associated paths through scanned Matterport 3D scenes from inside residential homes [24]. These datasets contain two distinct navigation challenges. The language instructions contain both object-centric references to landmarks and relative positional references to the current agent position. For example, ‘go to the blue chair, then turn left and stop at the wooden table’ versus ‘move forward and turn left and stop in the hallway’ respectively.

In this work, we investigate the capability of object-centric

<sup>1</sup>Work done during SR and KA’s internships. SR, DT, KA, JW and BB are with the Boston Dynamics AI Institute {dta, jw}@theaiinstitute.com

<sup>2</sup>SR and AC are with Simon Fraser University {sraychau, angelx}@sfu.ca

<sup>3</sup>KA is with University of Pennsylvania {kashton}@upenn.edu

<sup>4</sup>BB is with University of Michigan {bucherb}@umich.edu

instruction following alone. There is substantial value in disentangling these two challenges. This value can be understood from both a cognitive science and robotics perspective. Neuroscience researchers have found that distinct regions of the brain enable people to perform landmark-based spatial navigation using observed scene objects [1]. While successful artificial intelligence algorithms are frequently not a direct mimic of human neural function, roboticists also have a long history of managing landmark-based navigation [25] and relative positional navigation [26]–[28] with clearly distinct methodological approaches. This distinction in both biological systems and autonomous navigation algorithms motivates us to consider that successful language grounding for these different types of navigation may also be achieved with distinct methodologies.

**Contributions.** In this work, we present a vision-language navigation dataset of exclusively object-centric navigation instruction following commands (OC-VLN). We also propose natural language grounded SLAM (NL-SLAM) for grounding natural language navigation instructions to robot observations and poses. We present a novel navigation policy to actively perform NL-SLAM in order to follow natural language instructions on OC-VLN. Our novel methods, leveraging pre-trained vision and language foundation models, require no task-specific training. Finally, we demonstrate the viability of NL-SLAM to perform real-world navigation instruction following on a Boston Dynamics Spot robot.

## II. RELATED WORK

**Natural Language Grounding to Landmarks.** Recently there has been much interest in fusing information from 2D foundation models into 3D scene representations. Many approaches represent per-pixel semantic features using explicit representations such as pointclouds [29]–[35], or implicit neural representations [36]–[47]. For methods which plan over objects instead of dense features such scene representations necessitate extra storage and computation compared to object-centric representations. More similar to our approach, other methods [48], [49] use a 3D scene graph (3DSG) where nodes and edges represent objects and inter-object relationships, respectively. Unlike us, however, these methods do not consider pose uncertainty when constructing the 3DSG.

Kimera [9] is a SLAM method that creates a hierarchical scene representation, including a dynamic scene graph. They build this scene graph from a metric-semantic mesh, which is the base of their scene representation. Our method NL-SLAM is more lightweight as we only map task-relevant objects instead of the full geometry of the scene. Unlike these approaches NL-SLAM also incorporates prior knowledge of the scene layout obtained from the navigation instruction.

**Vision-Language Navigation.** In the Vision-and-Language Navigation (VLN) task [21]–[23], a robot follows a path described by dense natural language instructions. These instructions involve taking actions such as turning as well as referring to objects or regions. Two related indoor tasks, REVERIE [50] and SOON [51] provide a description of a specific object to locate. These tasks both describe the

end location rather than the full path. In contrast, our task OC-VLN describes an entire path in an object-centric way, supporting focused research on landmark-based navigation.

A fundamental challenge in both VLN and OC-VLN is how to align dense natural language instructions to a path in the real world. Trained methods can discover this alignment directly from image observations [52] or, more commonly, through leveraging map-based approaches [53]–[57]. However, these methods have struggled with sim-to-real transfer problems in the few cases where they have been run in the real world [58], [59]. Recently, much VLN research has focused on exploring the impact of the research advances in large language models (LLMs) and Vision-Language Model (VLMs) on the ability to solve VLN with zero-shot approaches [60]–[68]. Some zero-shot VLN methods demonstrated results in the real world [62], [68] where they outperformed trained approaches with good results in simulation. Some recent methods [65], [66] construct topological maps to store navigation history and information about the observed environment to support an LLM-based planner. Unlike these methods, our NL-SLAM uses an LLM not as a direct planner but instead to generate an inferred pose graph based on the instruction, allowing us to take advantage of established techniques from robotics to adjust this inferred pose graph according to the observed environment while using it to follow the specified path.

## III. DATASET

We introduce the Object-Centric VLN (OC-VLN) task, where a robot is required to navigate by following object-centric instructions to reach a target. Our task is similar to VLN [21] and VLN-CE [23], where the agent follows fine-grained instructions to reach a target (‘Go down the hallway, and take a right. Once you reach the bench on your right stop on the carpet.’). However, we focus on instructions that specify objects as landmarks (e.g., object-centric instructions). We use the same agent embodiment and task setting as VLN-CE.

**Dataset Generation.** We generate our episodes using real-world 3D scans from HM3DSem [69] in the Habitat simulator [70]. Goat-Bench [71] is a recently introduced dataset where an agent is tasked to navigate to a sequence of open-vocabulary objects specified via either a category name, an image or a language description. We use the trajectories in this dataset to generate fine-grained instructions using GPT-4 [15]. First, we use an oracle agent which follows the ground-truth trajectories and saves RGB images at each step. Next, we proceed to generate a navigation instruction that will enable an agent to reach from the start to the end of the trajectory. We do so in two stages – *Stage1*: we prompt GPT-4 with the RGB images from the first and last frames of the trajectory and ask it to extract key objects; *Stage2*: we then prompt GPT-4 with all the sequential images collected for the trajectory along with the object names from Stage1 and ask it to generate a fine-grained object-centric instruction.

**Statistics.** OC-VLN contains episodes spanning  $\sim 7$ m and having open-vocabulary language instructions (Fig. 2) with



	Waypoints	Actions	Landmarks	Relations
Move forward towards the red rug. Turn right and move towards the bench. Stop near the bench.	1. starting point 2. near red rug 3. after right turn 4. near bench 5. stopping point	1 → 2 move forward 2 → 3 turn right 3 → 4 move forward 4 → 5 stop	1. red rug 2. bench	1 → 2 near 2 → 4 near
Turn around. Move towards the closet. Move past the wall clock on your left.	1. starting point 2. after turning 3. near closet 4. near wall clock 5. stopping point	1 → 2 turn around 2 → 3 move forward 3 → 4 move forward 4 → 5 stop	1. closet 2. wall clock	1 → 3 near 2 → 4 left

Fig. 3: Using an LLM we extract waypoints, landmarks, waypoint-waypoint actions and landmark-waypoint relations.

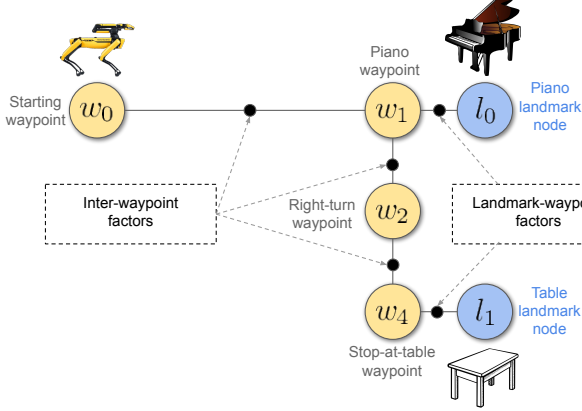


Fig. 4: **Language-inferred factor graph** derived from the instruction “Go forward to the piano, then turn right and stop at the table.”. See text for more details.

### B. SLAM with inferred map prior

Our framework integrates the language-inferred map prior into a traditional object-based SLAM navigation system. The prior map initially has high uncertainty due to the inherent ambiguity in linguistic descriptions and the lack of direct sensory information. As the robot navigates, it simultaneously localizes itself within this uncertain map while refining the map through observations, gradually transforming the vague linguistic description into a precise spatial representation.

The primary objective is to find the Maximum A Posteriori (MAP) estimate of the joint distribution over the robot poses  $X$ , observed landmarks  $O$ , language-inferred waypoints  $W$  and landmarks  $L$ , conditioned on all sensor observations  $Z$  and the linguistic descriptions of relationships among waypoints and landmarks  $R$ . Formally, this is expressed as:

$$X^*, O^*, W^*, L^* = \operatorname{argmax}_{X, O, W, L} p(X, O, W, L | Z, R)$$

which can be decomposed into two components:

$$p(X, O, W, L | Z, R) = p(X, O | Z) p(W, L | X, Z, R)$$

The first term,  $p(X, O | Z)$  is the traditional landmark-based SLAM problem, which can be efficiently solved using state-of-the-art SLAM algorithms [10], [11], [72]. The second term,  $p(W, L | X, Z, R)$ , incorporates the language-inferred map:

$$p(W, L | X, O, Z, R) \propto p(R | W, L) p(Z | L, X) \quad (2)$$

Here,  $p(R | W, L)$  is our inferred factor graph in eq. (1), and  $p(Z | L, X) = \prod_{ik} p(z_{jk} | l_j, x_k)$  are the landmark-observation likelihood factors, where  $z_{jk}$  is the observation associated with the inferred landmark  $l_j$  when the robot is at pose  $x_k$ . These factors are essential for reducing uncertainty in the inferred landmarks, subsequently enhancing the accuracy and reducing the uncertainty of the associated waypoints. The inferred graph augmented with landmark-observation factors can be efficiently optimized using standard factor graph SLAM packages, e.g., [73], allowing us to leverage established SLAM solutions while integrating our novel language-informed priors with real sensory observations.

### C. Data association of inferred landmarks and observations

To create the landmark-observation factors  $p(z_{jk} | l_j, x_k)$  in eq. (2), we must perform data association between the inferred landmarks and the observations. In this context, a landmark could have multiple candidate observation matches, and one observation could potentially match multiple landmarks. While this data association problem could be solved using Expectation-Maximization (EM) [74], [75] or hybrid inference on a discrete-continuous factor graph [76], we opt for a simpler approach. Our method matches landmarks with observations pairwise, selecting the best match with cosine similarity between their CLIP [18] text features:

$$l^* = \operatorname{argmax}_l [\operatorname{cosine\_sim}(\mathcal{F}_t(l), \mathcal{F}_o(z))] \quad (3)$$

where  $\mathcal{F}_t(\cdot)$  provides text features by encoding the landmark name in the inferred graph, and  $\mathcal{F}_o(\cdot)$  gives text features of the observation. If the similarity is below a threshold no association is made. This approach offers a balance between effectiveness and computational efficiency. Future iterations of the system may explore more sophisticated data association techniques to handle ambiguous cases.

### D. Navigation Policy

Localizing the robot within the language-inferred map enables a straightforward navigation policy: The robot navigates by sequentially moving to inferred waypoints, transitioning when within 0.5m of each, and stopping at the last one. However, high uncertainty in waypoint locations can lead to inaccurate navigation. In these cases, the robot should switch to exploration mode, seeking landmarks to reduce uncertainty about upcoming waypoints.

To balance exploration and exploitation, we employ the following strategy for waypoint selection:

$$w^* = \operatorname{argmin}_{w_j \forall j} [||w_j \ominus x_i||^2 + \alpha \operatorname{trace}(\Lambda_{w_j})] \quad (4)$$

This equation selects the inferred waypoint  $w_j$  that minimizes two factors: the distance between the waypoint and the current robot pose ( $||w_j \ominus x_i||^2$ ), and the uncertainty of the waypoint, represented by the trace of its information matrix  $\Lambda = \Sigma^{-1}$ . The weighting constant  $\alpha$  balances the desire to move towards nearby waypoints with the need to reduce uncertainty.

To determine the precise navigation target, we further sample a point from the posterior distribution  $p(w^*)$  within

the navigable region around  $w^*$ . Initially, the posterior distributions of waypoints have high uncertainty, promoting exploration. As the robot gathers observations, uncertainty decreases, refining navigation targets. This adaptive approach allows the robot to navigate efficiently while continuously improving its spatial understanding.

## V. EXPERIMENTS

**Metrics.** We use the commonly used evaluation metrics for VLN [21], [77], [78], such as Success Rate (SR), Success weighted by inverse Path Length (SPL), Oracle Success Rate (OSR), and normalized Dynamic-Time Warping (nDTW). The first three metrics measure the robot’s performance based on how well it can reach the target object, while nDTW measures how closely it can follow the instructions.

**Implementation.** We evaluate NL-SLAM on OC-VLN in the Habitat simulator [70] in a zero-shot manner. We use a pipeline of pre-trained open-vocabulary object detection for landmark recognition. Given an RGB image, we use RAM [79] for identifying what objects are in the image, Grounding-Dino [19] to predict bounding boxes, and finally, Segment-Anything (SAM) [20] to obtain the semantic segmentation. For the navigator, we use a PointNav policy [80] pre-trained on HM3D [81] scenes. We compare our method to two baselines, both SOTA zero-shot navigation methods for related tasks that have been successful in the real world.

**Seq-VLFM baseline.** VLFM [82] is an Object-Goal navigation method, which we execute sequentially. We use GPT-4 [15] to extract the objects from the instruction and then run VLFM to go to each object in order. Using BLIP-2 [83], VLFM creates value maps of likely object locations, guiding the frontier-based exploration [84] to efficiently find objects.

**InstructNav baseline.** InstructNav [85] is a method for general navigation instruction following which evaluates on Object-Goal navigation, VLN, and demand-driven navigation tasks. InstructNav uses an LLM to break the navigation instruction down into a series of paired actions and landmarks. It then plans how to reach each landmark using a combination of value maps, which represent key information about the environment and its relation to the robot, such as semantic information, actions, trajectory history, and intuition from the LLM. They replan with the LLM at each decision-making step to better fit the plan to the observed environment.

## VI. RESULTS

**Benchmark results.** Table II shows that NL-SLAM outperforms the baseline methods on all metrics. Our performance on the nDTW metric (48%) specifically indicates that our method is able to follow instructions better than the others. This is intuitive since our method transforms the instructions into a graph, which is then used to perform the navigation, compared to Seq-VLFM, which searches for objects by extracting them from the instructions and thus disregarding the actions and relations encoded into them. Being able to follow the instructions also enables NL-SLAM to successfully reach the target object by following the suggested path as indicated by its performance on the SR and SPL metrics. The OSR

metric reflects whether the agent has been near the target object and failed to stop. We find that all the methods achieve reasonable OSR on the dataset. However, the gap between SR and OSR is smaller for NL-SLAM (20%) compared to the others (42% in Seq-VLFM and 43% in InstructNav), indicating that our method is able to call the *Stop* action correctly more often compared to the others.

TABLE II: **Performance.** NL-SLAM significantly outperforms Seq-VLFM and InstructNav on all metrics.

Method	SR	SPL	OSR	nDTW
Seq-VLFM	0.33	0.24	0.75	0.33
InstructNav	0.24	0.07	0.67	0.33
NL-SLAM (Ours)	<b>0.58</b>	<b>0.40</b>	<b>0.78</b>	<b>0.48</b>

**Qualitative analysis.** In Fig. 5, we visualize our agent performance on a single episode over time. At the beginning of the episode ( $t = 1$ ), when the agent has not yet made observations in the world, the landmark nodes ( $l_i = \{l_1 = \text{“brown couch”}, l_2 = \text{“fireplace”}\}$ ) and the waypoint nodes ( $w_i = \{w_2, w_3\}$ ) have large uncertainties (visualized as ellipses). As the episode progresses, the agent makes the first observation at  $t = 20$  and grounds  $l_1$  and  $w_1$ , thereby becoming certain about their locations. At  $t = 50$ , the agent observes  $l_2$ , thus reducing uncertainty for all the nodes in the inferred graph. Finally, the agent generates the *Stop* action when it is within 0.5m of the last waypoint  $w_2$  in the graph.

To compare NL-SLAM and Seq-VLFM, we visualize the agent trajectories for different episodes (Fig. 6) and observe that the agent follows the instruction better in NL-SLAM compared to Seq-VLFM. This is evident from how closely the agent path matches the ground-truth path in our method.

**Ablations.** We perform ablations on the different modules in NL-SLAM (Table III) to understand the contribution of each. For both *Object Detector* and *Navigator*, we find using an Oracle performs the best, as is expected. The Oracle detector+navigator achieves a +12% increase in success, +13% increase in SPL, and +10% increase in nDTW, indicating that the performance of our method is limited by the choice of the detector and the navigator and can be improved further.

TABLE III: **Ablations.** Oracle versions of the *Object Detector* and the *Navigator* perform better than the pre-trained models, indicating the scope of improvement for NL-SLAM.

Object Detector	Navigator	SR	SPL	OSR	nDTW
Oracle	Oracle	<b>0.70</b>	<b>0.53</b>	<b>0.80</b>	<b>0.58</b>
RAM+GDino+SAM	Oracle	0.67	0.48	<b>0.80</b>	0.53
RAM+GDino+SAM	PointNav	0.58	0.40	0.78	0.48

**Failure analysis.** We note two main failure cases: (a) the presence of multiple instances of the same object category; and (b) the misclassification of an object. In the first case, an instruction ‘move through an open door’ while there are multiple doors (Fig. 7) makes it difficult for the agent to figure out the correct ‘door’. The second case is a limitation of the

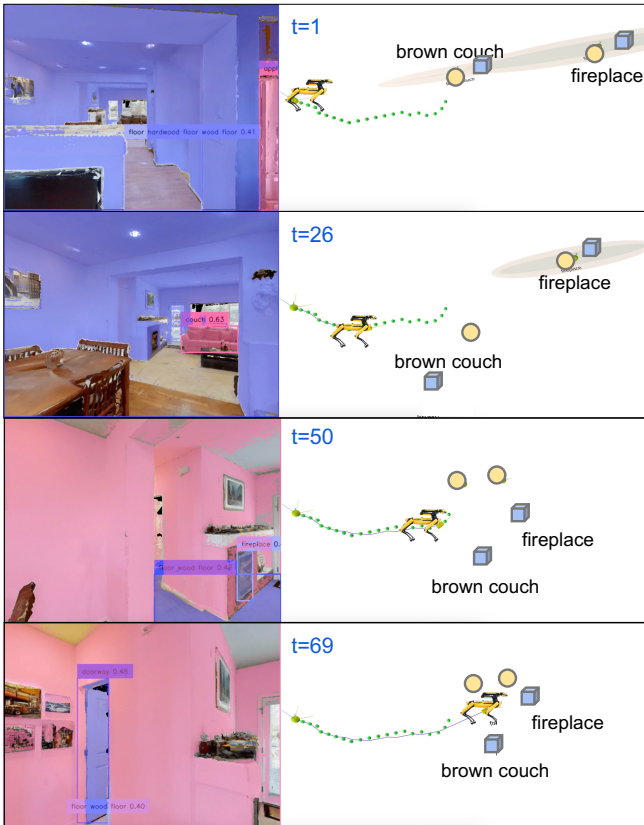


Fig. 5: **NL-SLAM in action.** Visualizing the progress of our agent through an episode shows how the *language-inferred graph* gets optimized over time  $t$ , leading to a successful completion. (left) shows detected objects; (right) shows current robot pose, ground-truth trajectory (green), inferred waypoints (yellow) and landmarks (blue).

object detector where it incorrectly identifies a ‘television’ as ‘fireplace’, leading to erroneous data association.

**Real-world demonstrations.** We deployed NL-SLAM on a Spot robot from Boston Dynamics to demonstrate its effectiveness in the real world. We replaced the PointNav policy with the Boston Dynamics Spot SDK as the navigator to move the robot to a waypoint. We use RTAB-Map to obtain the robot’s coordinates and the observations in a reference frame. Instead of our object detection pipeline, we use YOLOv7 [86] for faster real-time execution. We ran NL-SLAM in an office space with commonly occurring objects such as chairs, tables, potted plants, etc., and demonstrated that our method was able to perform well in this task.

## VII. CONCLUSION

We present OC-VLN, a dataset for object-centric vision-and-language navigation enabling us to study the distinct challenge of object-based navigation instruction following. To address this task, we propose NL-SLAM, which robustly grounds objects in the instruction to observations in the environment using a pose graph. NL-SLAM creates an inferred pose graph from the instruction using an LLM, thus incorporating relevant information as a prior for the pose graph. A comparison to two baselines, Seq-VLFM [82] and

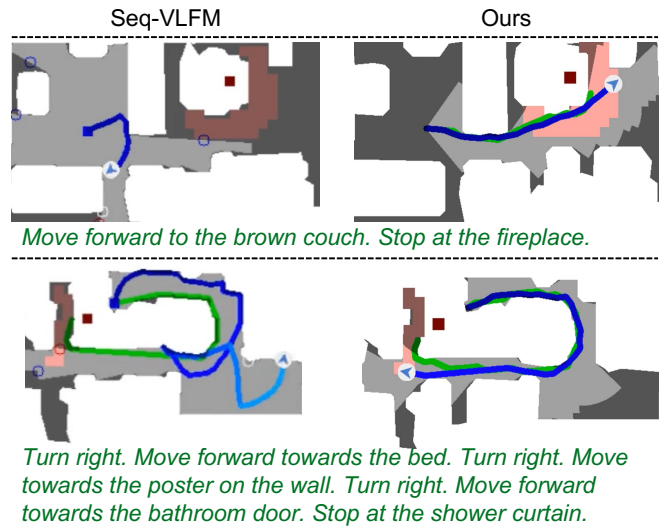


Fig. 6: **Comparison.** Our agent (right) trajectory aligns with the ground-truth trajectory better than Seq-VLFM (left), indicating better instruction following ability. Agent trajectory is blue, ground-truth path is green and target object is red.

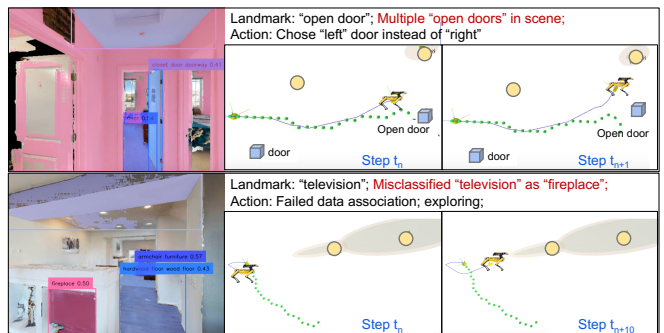


Fig. 7: **Failure cases.** Two frequent failure cases in NL-SLAM are: (top) multiple instances of the same landmark present, e.g. ‘door’; and (bottom) an object is mis-classified e.g. ‘television’ identified as ‘fireplace’.

InstructNav [85], which are SOTA on related tasks, shows that NL-SLAM outperforms them on all metrics.

NL-SLAM can struggle to identify the relevant objects when multiple of the same class are present. This could be addressed by incorporating scene layout priors to predict likely locations for landmarks that have not yet been observed and thus identifying promising directions for the path as a whole. Actively selecting poses to obtain multiple good views of the object, perhaps drawing inspiration from active SLAM, is an avenue to address the other significant cause of failure identified for NL-SLAM, i.e. object misclassification. More sophisticated data association techniques may also alleviate these limitations.

While object-centric vision-and-language navigation is far from solved as a distinct problem, future work should also investigate modularly including more aspects present in VLN. For example, regions as landmarks as well as objects.

## REFERENCES

- [1] E. Chan, O. Baumann, M. Bellgrove, and J. Mattingley, "From objects to landmarks: The function of visual location information in spatial navigation," *Frontiers in Psychology*, vol. 3, p. 304, 08 2012.
- [2] G. Janzen and M. Van Turenout, "Selective neural representation of objects relevant for navigation," *Nature neuroscience*, vol. 7, no. 6, pp. 673–677, 2004.
- [3] P. Foo, W. H. Warren, A. Duchon, and M. J. Tarr, "Do humans integrate routes into a cognitive map? map-versus landmark-based navigation of novel shortcuts," *Journal of Experimental Psychology: Learning, Memory, and Cognition*, vol. 31, no. 2, p. 195, 2005.
- [4] V. R. Schinazi and R. A. Epstein, "Neural correlates of real-world route learning," *Neuroimage*, vol. 53, no. 2, pp. 725–735, 2010.
- [5] S. Thrun and M. Montemerlo, "The graph slam algorithm with applications to large-scale mapping of urban structures," *The International Journal of Robotics Research*, vol. 25, no. 5-6, pp. 403–429, 2006.
- [6] R. Mur-Artal and J. D. Tardós, "Orb-slam2: An open-source slam system for monocular, stereo, and rgb-d cameras," *IEEE transactions on robotics*, vol. 33, no. 5, pp. 1255–1262, 2017.
- [7] C. Campos, R. Elvira, J. J. G. Rodríguez, J. M. Montiel, and J. D. Tardós, "Orb-slam3: An accurate open-source library for visual, visual-inertial, and multimap slam," *IEEE Transactions on Robotics*, vol. 37, no. 6, pp. 1874–1890, 2021.
- [8] A. Rosinol, M. Abate, Y. Chang, and L. Carlone, "Kimera: an open-source library for real-time metric-semantic localization and mapping," in *2020 IEEE International Conference on Robotics and Automation (ICRA)*. IEEE, 2020, pp. 1689–1696.
- [9] A. Rosinol, A. Violette, M. Abate, N. Hughes, Y. Chang, J. Shi, A. Gupta, and L. Carlone, "Kimera: From SLAM to spatial perception with 3D dynamic scene graphs," *The International Journal of Robotics Research*, vol. 40, no. 12-14, pp. 1510–1546, 2021.
- [10] M. Labbé and F. Michaud, "Rtab-map as an open-source lidar and visual simultaneous localization and mapping library for large-scale and long-term online operation," *Journal of field robotics*, vol. 36, no. 2, pp. 416–446, 2019.
- [11] J. A. Placed, J. Strader, H. Carrillo, N. Atanasov, V. Indelman, L. Carlone, and J. A. Castellanos, "A survey on active simultaneous localization and mapping: State of the art and new frontiers," *IEEE Transactions on Robotics*, vol. 39, no. 3, pp. 1686–1705, 2023.
- [12] W. Knight, "With a roomba capable of navigation, irobot eyes advanced home robots," *MIT Technology Review*, 2015.
- [13] E. Eade, P. Fong, and M. E. Munich, "Monocular graph slam with complexity reduction," in *2010 IEEE/RSJ International Conference on Intelligent Robots and Systems*. IEEE, 2010, pp. 3017–3024.
- [14] E. Ackerman, "Exyn brings level 4 autonomy to drones," *IEEE Spectrum*, 2021.
- [15] OpenAI, "Gpt-4 technical report," 2023.
- [16] J. Li, D. Li, S. Savarese, and S. Hoi, "BLIP-2: bootstrapping language-image pre-training with frozen image encoders and large language models," in *ICML*, 2023.
- [17] H. Liu, C. Li, Q. Wu, and Y. J. Lee, "Visual instruction tuning," *Advances in neural information processing systems*, vol. 36, 2024.
- [18] A. Radford, J. W. Kim, C. Hallacy, A. Ramesh, G. Goh, S. Agarwal, G. Sastry, A. Askell, P. Mishkin, J. Clark, *et al.*, "Learning transferable visual models from natural language supervision," in *International conference on machine learning*. PMLR, 2021, pp. 8748–8763.
- [19] S. Liu, Z. Zeng, T. Ren, F. Li, H. Zhang, J. Yang, C. Li, J. Yang, H. Su, J. Zhu, *et al.*, "Grounding dino: Marrying dino with grounded pre-training for open-set object detection," *arXiv preprint arXiv:2303.05499*, 2023.
- [20] A. Kirillov, E. Mintun, N. Ravi, H. Mao, C. Rolland, L. Gustafson, T. Xiao, S. Whitehead, A. C. Berg, W.-Y. Lo, *et al.*, "Segment anything," *arXiv preprint arXiv:2304.02643*, 2023.
- [21] P. Anderson, Q. Wu, D. Teney, J. Bruce, M. Johnson, N. Sünderhauf, I. Reid, S. Gould, and A. Van Den Hengel, "Vision-and-language navigation: Interpreting visually-grounded navigation instructions in real environments," in *Proceedings of the IEEE conference on computer vision and pattern recognition*, 2018, pp. 3674–3683.
- [22] A. Ku, P. Anderson, R. Patel, E. Ie, and J. Baldrige, "Room-across-room: Multilingual vision-and-language navigation with dense spatiotemporal grounding," *arXiv preprint arXiv:2010.07954*, 2020.
- [23] J. Krantz, E. Wijmans, A. Majumdar, D. Batra, and S. Lee, "Beyond the nav-graph: Vision-and-language navigation in continuous environments," in *Computer Vision—ECCV 2020: 16th European Conference, Glasgow, UK, August 23–28, 2020, Proceedings, Part XXVIII 16*. Springer, 2020, pp. 104–120.
- [24] A. Chang, A. Dai, T. Funkhouser, M. Halber, M. Niessner, M. Savva, S. Song, A. Zeng, and Y. Zhang, "Matterport3d: Learning from rgb-d data in indoor environments," *arXiv preprint arXiv:1709.06158*, 2017.
- [25] H. Durrant-Whyte and T. Bailey, "Simultaneous localization and mapping: part i," *IEEE robotics & automation magazine*, vol. 13, no. 2, pp. 99–110, 2006.
- [26] G. Sibley, C. Mei, I. Reid, and P. Newman, "Vast-scale outdoor navigation using adaptive relative bundle adjustment," *The International Journal of Robotics Research*, vol. 29, no. 8, pp. 958–980, 2010.
- [27] D. Sibley, C. Mei, I. D. Reid, and P. Newman, "Adaptive relative bundle adjustment," in *Robotics: science and systems*, vol. 32, 2009, p. 33.
- [28] S. Anderson, K. MacTavish, and T. D. Barfoot, "Relative continuous-time slam," *The International Journal of Robotics Research*, vol. 34, no. 12, pp. 1453–1479, 2015.
- [29] K. M. Jatavallabhula, A. Kuwajerwala, Q. Gu, M. Omama, T. Chen, A. Maalouf, S. Li, G. Iyer, S. Saryazdi, N. Keetha, *et al.*, "Conceptfusion: Open-set multimodal 3d mapping," *arXiv preprint arXiv:2302.07241*, 2023.
- [30] S. Peng, K. Genova, C. M. Jiang, A. Tagliasacchi, M. Pollefeys, and T. Funkhouser, "Openscene: 3d scene understanding with open vocabularies," in *Proceedings of the IEEE/CVF Conference on Computer Vision and Pattern Recognition (CVPR)*, 2023.
- [31] R. Ding, J. Yang, C. Xue, W. Zhang, S. Bai, and X. Qi, "Lowis3d: Language-driven open-world instance-level 3d scene understanding," *IEEE Transactions on Pattern Analysis and Machine Intelligence*, 2024.
- [32] —, "Pla: Language-driven open-vocabulary 3d scene understanding," in *Proceedings of the IEEE/CVF conference on computer vision and pattern recognition*, 2023, pp. 7010–7019.
- [33] J. Zhang, R. Dong, and K. Ma, "Clip-fo3d: Learning free open-world 3d scene representations from 2d dense clip," in *Proceedings of the IEEE/CVF International Conference on Computer Vision*, 2023, pp. 2048–2059.
- [34] B. Chen, F. Xia, B. Ichter, K. Rao, K. Gopalakrishnan, M. S. Ryoo, A. Stone, and D. Kappler, "Open-vocabulary queryable scene representations for real world planning," in *2023 IEEE International Conference on Robotics and Automation (ICRA)*. IEEE, 2023, pp. 11 509–11 522.
- [35] L. Jiang, S. Shi, and B. Schiele, "Open-vocabulary 3D semantic segmentation with foundation models," in *Proceedings of the IEEE/CVF Conference on Computer Vision and Pattern Recognition*, 2024, pp. 21 284–21 294.
- [36] V. Tschernezki, I. Laina, D. Larlus, and A. Vedaldi, "Neural feature fusion fields: 3d distillation of self-supervised 2d image representations," in *2022 International Conference on 3D Vision (3DV)*. IEEE, 2022, pp. 443–453.
- [37] S. Kobayashi, E. Matsumoto, and V. Sitzmann, "Decomposing nerf for editing via feature field distillation," *Advances in Neural Information Processing Systems*, vol. 35, pp. 23 311–23 330, 2022.
- [38] N. M. M. Shafiqullah, C. Paxton, L. Pinto, S. Chintala, and A. Szlam, "Clip-fields: Weakly supervised semantic fields for robotic memory," in *Conference on Robot Learning Workshops*, 2022.
- [39] N. Tsagkas, O. Mac Aodha, and C. X. Lu, "VL-Fields: Towards language-grounded neural implicit spatial representations," in *International Conference on Robotics and Automation Workshops*, 2023.
- [40] J. Kerr, C. M. Kim, K. Goldberg, A. Kanazawa, and M. Tancik, "LeRF: Language embedded radiance fields," in *Proceedings of the IEEE/CVF International Conference on Computer Vision*, 2023, pp. 19 729–19 739.
- [41] C. Huang, O. Mees, A. Zeng, and W. Burgard, "Audio visual language maps for robot navigation," in *International Symposium on Experimental Robotics*. Springer, 2023, pp. 105–117.
- [42] W. Shen, G. Yang, A. Yu, J. Wong, L. P. Kaelbling, and P. Isola, "Distilled feature fields enable few-shot language-guided manipulation," in *Conference on Robot Learning*, 2023.
- [43] F. Engelmann, F. Manhardt, M. Niemeyer, K. Tateno, M. Pollefeys, and F. Tombari, "OpenNeRF: Open Set 3D Neural Scene Segmentation with Pixel-Wise Features and Rendered Novel Views," in *International Conference on Learning Representations*, 2024.
- [44] K. Mazur, E. Sucar, and A. J. Davison, "Feature-realistic neural fusion for real-time, open set scene understanding," in *2023 IEEE*

- International Conference on Robotics and Automation (ICRA)*. IEEE, 2023, pp. 8201–8207.
- [45] R.-Z. Qiu, Y. Hu, G. Yang, Y. Song, Y. Fu, J. Ye, J. Mu, R. Yang, N. Atanasov, S. Scherer, and X. Wang, “Learning generalizable feature fields for mobile manipulation,” *arXiv preprint arXiv:2403.07563*, 2024.
- [46] J.-C. Shi, M. Wang, H.-B. Duan, and S.-H. Guan, “Language embedded 3D Gaussians for open-vocabulary scene understanding,” in *Proceedings of the IEEE/CVF Conference on Computer Vision and Pattern Recognition*, 2024, pp. 5333–5343.
- [47] K. Yamazaki, T. Hanyu, K. Vo, T. Pham, M. Tran, G. Doretto, A. Nguyen, and N. Le, “Open-fusion: Real-time open-vocabulary 3D mapping and queryable scene representation,” in *2024 IEEE International Conference on Robotics and Automation (ICRA)*. IEEE, 2024, pp. 9411–9417.
- [48] Q. Gu, A. Kuwajerwala, S. Morin, K. M. Jatavallabhula, B. Sen, A. Agarwal, C. Rivera, W. Paul, K. Ellis, R. Chellappa, et al., “Conceptgraphs: Open-vocabulary 3d scene graphs for perception and planning,” in *2024 IEEE International Conference on Robotics and Automation (ICRA)*. IEEE, 2024, pp. 5021–5028.
- [49] S. Koch, N. Vaskevicius, M. Colosi, P. Hermosilla, and T. Ropinski, “Open3DSG: Open-vocabulary 3D scene graphs from point clouds with queryable objects and open-set relationships,” in *Proceedings of the IEEE/CVF Conference on Computer Vision and Pattern Recognition (CVPR)*, June 2024.
- [50] Y. Qi, Q. Wu, P. Anderson, X. Wang, W. Y. Wang, C. Shen, and A. v. d. Hengel, “Reverie: Remote embodied visual referring expression in real indoor environments,” in *Proceedings of the IEEE/CVF Conference on Computer Vision and Pattern Recognition*, 2020, pp. 9982–9991.
- [51] F. Zhu, X. Liang, Y. Zhu, Q. Yu, X. Chang, and X. Liang, “Soon: Scenario oriented object navigation with graph-based exploration,” in *Proceedings of the IEEE/CVF Conference on Computer Vision and Pattern Recognition*, 2021, pp. 12 689–12 699.
- [52] A. Majumdar, A. Shrivastava, S. Lee, P. Anderson, D. Parikh, and D. Batra, “Improving vision-and-language navigation with image-text pairs from the web,” in *Computer Vision—ECCV 2020: 16th European Conference, Glasgow, UK, August 23–28, 2020, Proceedings, Part VI 16*. Springer, 2020, pp. 259–274.
- [53] S. Chen, P.-L. Gudur, M. Tapaswi, C. Schmid, and I. Laptev, “Think global, act local: Dual-scale graph transformer for vision-and-language navigation,” in *Proceedings of the IEEE/CVF Conference on Computer Vision and Pattern Recognition*, 2022, pp. 16 537–16 547.
- [54] Z. Wang, X. Li, J. Yang, Y. Liu, and S. Jiang, “Gridmm: Grid memory map for vision-and-language navigation,” in *Proceedings of the IEEE/CVF International Conference on Computer Vision*, 2023, pp. 15 625–15 636.
- [55] D. An, Y. Qi, Y. Li, Y. Huang, L. Wang, T. Tan, and J. Shao, “Bebert: Multimodal map pre-training for language-guided navigation,” in *Proceedings of the IEEE/CVF International Conference on Computer Vision*, 2023, pp. 2737–2748.
- [56] G. Georgakis, K. Schmeckpeper, K. Wanchoo, S. Dan, E. Mitsakaki, D. Roth, and K. Daniilidis, “Cross-modal map learning for vision and language navigation,” in *Proceedings of the IEEE/CVF Conference on Computer Vision and Pattern Recognition*, 2022, pp. 15 460–15 470.
- [57] R. Liu, W. Wang, and Y. Yang, “Volumetric environment representation for vision-language navigation,” in *Proceedings of the IEEE/CVF Conference on Computer Vision and Pattern Recognition*, 2024, pp. 16 317–16 328.
- [58] P. Anderson, A. Shrivastava, J. Truong, A. Majumdar, D. Parikh, D. Batra, and S. Lee, “Sim-to-real transfer for vision-and-language navigation,” in *Conference on Robot Learning*. PMLR, 2021, pp. 671–681.
- [59] T. Gervet, S. Chintala, D. Batra, J. Malik, and D. S. Chaplot, “Navigating to objects in the real world,” *Science Robotics*, vol. 8, no. 79, p. eadf6991, 2023.
- [60] V. S. Dorbala, G. Sigurdsson, R. Piramuthu, J. Thomason, and G. S. Sukhatme, “Clip-nav: Using clip for zero-shot vision-and-language navigation,” *arXiv preprint arXiv:2211.16649*, 2022.
- [61] G. Zhou, Y. Hong, and Q. Wu, “Navgpt: Explicit reasoning in vision-and-language navigation with large language models,” *arXiv preprint arXiv:2305.16986*, 2023.
- [62] Y. Long, X. Li, W. Cai, and H. Dong, “Discuss before moving: Visual language navigation via multi-expert discussions,” *arXiv preprint arXiv:2309.11382*, 2023.
- [63] D. Li, W. Chen, and X. Lin, “Tina: Think, interaction, and action framework for zero-shot vision language navigation,” *arXiv preprint arXiv:2403.08833*, 2024.
- [64] B. Lin, Y. Nie, Z. Wei, J. Chen, S. Ma, J. Han, H. Xu, X. Chang, and X. Liang, “Navcot: Boosting llm-based vision-and-language navigation via learning disentangled reasoning,” *arXiv preprint arXiv:2403.07376*, 2024.
- [65] J. Chen, B. Lin, R. Xu, Z. Chai, X. Liang, and K.-Y. K. Wong, “Mapgpt: Map-guided prompting for unified vision-and-language navigation,” *arXiv preprint arXiv:2401.07314*, 2024.
- [66] Z. Zhan, L. Yu, S. Yu, and G. Tan, “Mc-gpt: Empowering vision-and-language navigation with memory map and reasoning chains,” *arXiv preprint arXiv:2405.10620*, 2024.
- [67] C. Huang, O. Mees, A. Zeng, and W. Burgard, “Visual language maps for robot navigation,” in *2023 IEEE International Conference on Robotics and Automation (ICRA)*. IEEE, 2023, pp. 10 608–10 615.
- [68] C. Xu, H. T. Nguyen, C. Amato, and L. L. Wong, “Vision and language navigation in the real world via online visual language mapping,” *arXiv preprint arXiv:2310.10822*, 2023.
- [69] K. Yadav, R. Ramrakhya, S. K. Ramakrishnan, T. Gervet, J. Turner, A. Gokaslan, N. Maestre, A. X. Chang, D. Batra, M. Savva, et al., “Habitat-matterport 3d semantics dataset,” in *Proceedings of the IEEE/CVF Conference on Computer Vision and Pattern Recognition*, 2023, pp. 4927–4936.
- [70] M. Savva, A. Kadian, O. Maksymets, Y. Zhao, E. Wijmans, B. Jain, J. Straub, J. Liu, V. Koltun, J. Malik, et al., “Habitat: A platform for embodied ai research,” in *Proceedings of the IEEE/CVF international conference on computer vision*, 2019, pp. 9339–9347.
- [71] M. Khanna, R. Ramrakhya, G. Chhablani, S. Yenamandra, T. Gervet, M. Chang, Z. Kira, D. S. Chaplot, D. Batra, and R. Mottaghi, “Goat-bench: A benchmark for multi-modal lifelong navigation,” in *Proceedings of the IEEE/CVF Conference on Computer Vision and Pattern Recognition*, 2024, pp. 16 373–16 383.
- [72] F. Dellaert, M. Kaess, et al., “Factor graphs for robot perception,” *Foundations and Trends® in Robotics*, vol. 6, no. 1-2, pp. 1–139, 2017.
- [73] F. Dellaert and G. Contributors, “borglab/gtsam,” May 2022. [Online]. Available: <https://github.com/borglab/gtsam>
- [74] F. Dellaert, S. Seitz, S. Thrun, and C. Thorpe, “Feature correspondence: A markov chain monte carlo approach,” *Advances in Neural Information Processing Systems*, vol. 13, 2000.
- [75] S. L. Bowman, N. Atanasov, K. Daniilidis, and G. J. Pappas, “Probabilistic data association for semantic slam,” in *2017 IEEE international conference on robotics and automation (ICRA)*. IEEE, 2017, pp. 1722–1729.
- [76] K. J. Doherty, Z. Lu, K. Singh, and J. J. Leonard, “Discrete-continuous smoothing and mapping,” *IEEE Robotics and Automation Letters*, vol. 7, no. 4, pp. 12 395–12 402, 2022.
- [77] P. Anderson, A. Chang, D. S. Chaplot, A. Dosovitskiy, S. Gupta, V. Koltun, J. Kosecka, J. Malik, R. Mottaghi, and M. Savva, “On evaluation of embodied navigation agents,” *arXiv preprint arXiv:1807.06757*, 2018.
- [78] G. Ilharco, V. Jain, A. Ku, E. Ie, and J. Baldridge, “General evaluation for instruction conditioned navigation using dynamic time warping,” *arXiv preprint arXiv:1907.05446*, 2019.
- [79] Y. Zhang, X. Huang, J. Ma, Z. Li, Z. Luo, Y. Xie, Y. Qin, T. Luo, Y. Li, S. Liu, et al., “Recognize anything: A strong image tagging model,” in *Proceedings of the IEEE/CVF Conference on Computer Vision and Pattern Recognition*, 2024, pp. 1724–1732.
- [80] E. Wijmans, A. Kadian, A. Morcos, S. Lee, I. Essa, D. Parikh, M. Savva, and D. Batra, “Dd-ppo: Learning near-perfect pointgoal navigators from 2.5 billion frames,” in *International Conference on Learning Representations*.
- [81] S. K. Ramakrishnan, A. Gokaslan, E. Wijmans, O. Maksymets, A. Clegg, J. M. Turner, E. Undersander, W. Galuba, A. Westbury, A. X. Chang, M. Savva, Y. Zhao, and D. Batra, “Habitat-matterport 3D dataset (HM3d): 1000 large-scale 3D environments for embodied AI,” in *NeurIPS Datasets and Benchmarks Track (Round 2)*, 2021.
- [82] N. Yokoyama, S. Ha, D. Batra, J. Wang, and B. Bucher, “Vfm: Vision-language frontier maps for zero-shot semantic navigation,” *2024 IEEE International Conference on Robotics and Automation (ICRA)*, 2024.
- [83] J. Li, D. Li, S. Savarese, and S. Hoi, “Blip-2: Bootstrapping language-image pre-training with frozen image encoders and large language models,” in *International conference on machine learning*. PMLR, 2023, pp. 19 730–19 742.

- [84] B. Yamauchi, "A frontier-based approach for autonomous exploration," in *Proceedings 1997 IEEE International Symposium on Computational Intelligence in Robotics and Automation CIRA'97. Towards New Computational Principles for Robotics and Automation*. IEEE, 1997, pp. 146–151.
- [85] Y. Long, W. Cai, H. Wang, G. Zhan, and H. Dong, "Instructnav: Zero-shot system for generic instruction navigation in unexplored environment," *CoRL*, 2024.
- [86] C.-Y. Wang, A. Bochkovskiy, and H.-Y. M. Liao, "Yolov7: Trainable bag-of-freebies sets new state-of-the-art for real-time object detectors," in *Proceedings of the IEEE/CVF conference on computer vision and pattern recognition*, 2023, pp. 7464–7475.